Wide field polarization calibration in the image plane using the ATA

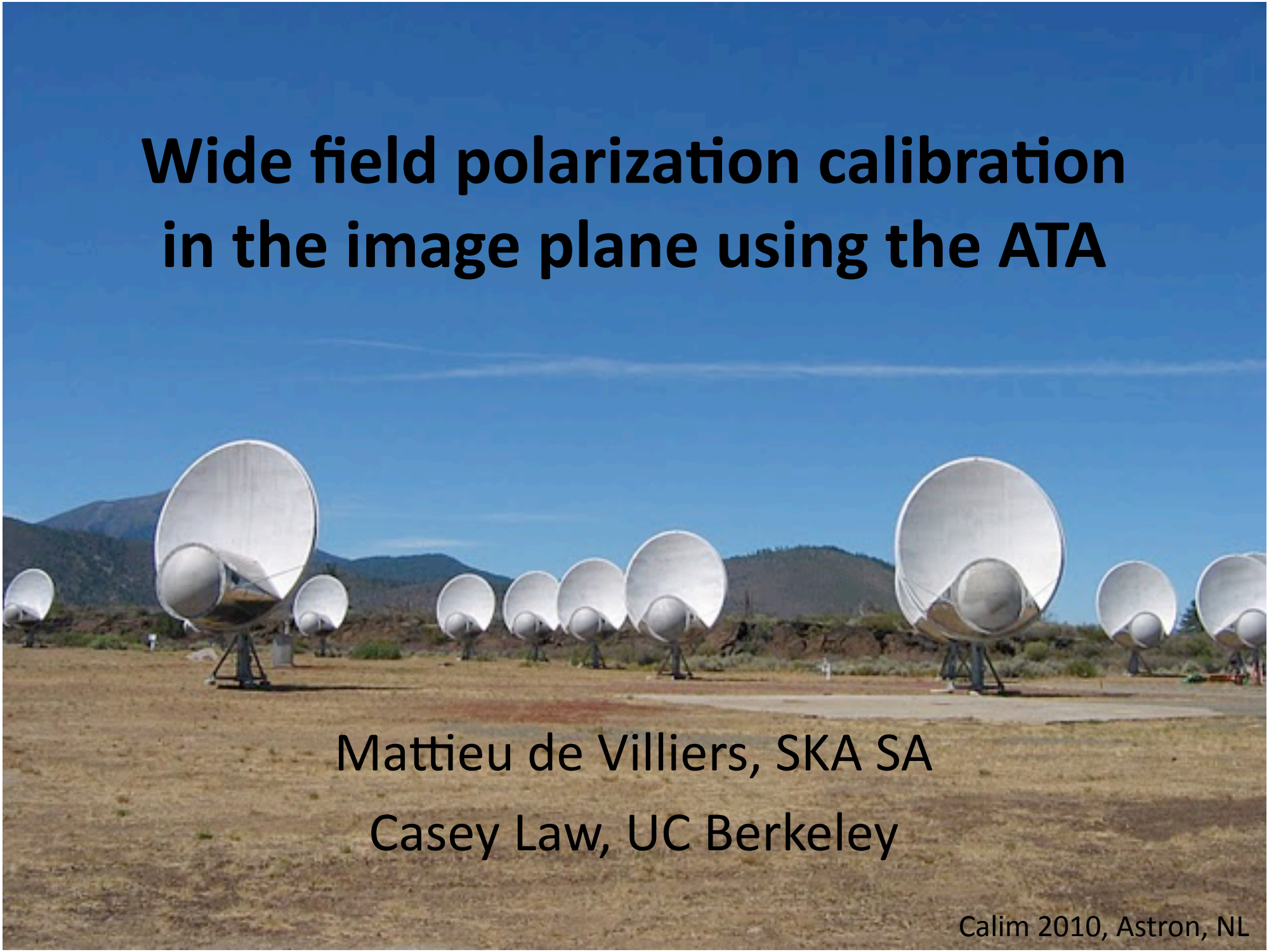

Mattieu de Villiers, SKA SA

Casey Law, UC Berkeley

Calim 2010, Astron, NL

Overview

- Background and goals
- Description of dataset
- Initial imaging results
- Calibration solutions
- Relative AZ EL plane
- Modeling direction dependent terms
- Prediction results
- Conclusions

Faceting (mosaicing within the FoV)

Independent calibration solutions per antenna, frequency, pointing

Image plane modeling and correction

Model overall direction dependent interferometer polarimetric response on top of standard center field calibration

Background / Goals

- Investigate polarization calibration over a wide field of view and wide bandwidth for the ATA
  - Using Miriad (Miriad is integrated into the ATA)
  - Seek solution requiring minimal modification to Miriad
  - Attempt a first order correction, not 1:1E6 dynamic range
- Discussed in this talk:
  - Investigate primary beam effects on calibration solutions
  - Model the effects (for making corrections to first order)
- Longer term goals:
  - Explore time stability of solutions
  - Devise a practical calibration strategy to remove wide FOV and wide bandwidth effects

Observation Dataset

- 17 pointings are observed using the ATA in a cross pattern towards linear polarization calibrator 3C286
- At extreme pointings, 3C286 lies at half the distance to the half power point of the primary beam
- 100MHz bandwidth are observed in 1024 channels, around 3.14GHz
- Each pointing is scanned for 50s in turn. This sequence is repeated 8 times
- 28 of the 42 alt az antennas of the ATA were used
- Dish diameter: 6m

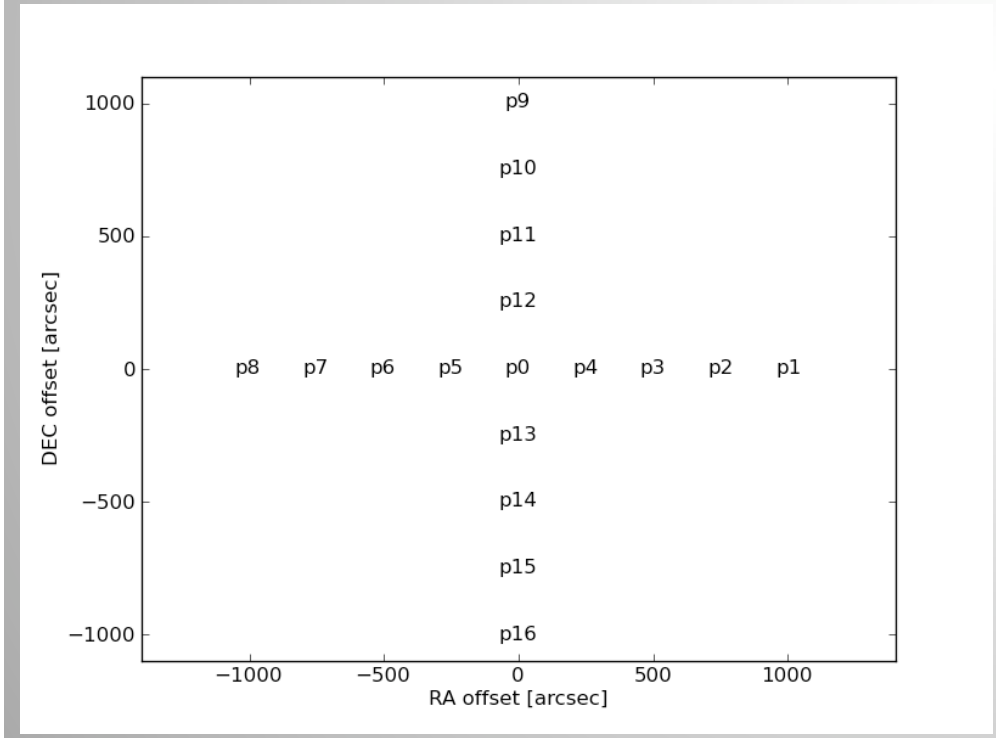

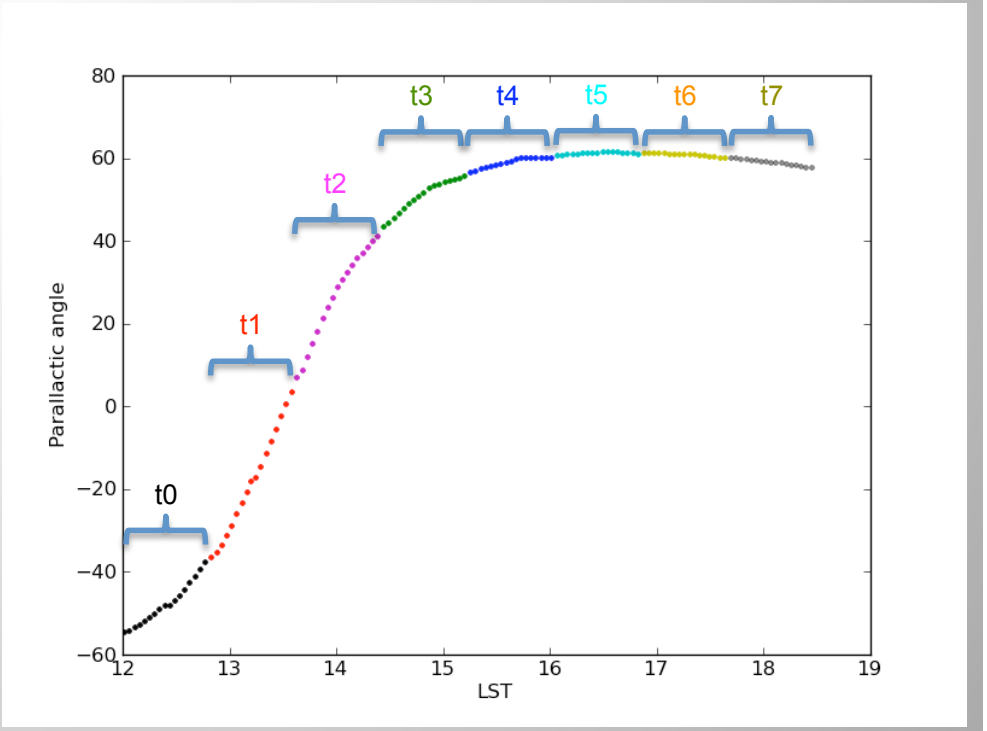

Direct solution for IQUV by calibrating central pointing

- Calibrated for pointing p0 only, including
  - Bandpass calibration
  - Gain calibration (in 8 time intervals)
  - Polarization calibration (X,Y leakages per antenna)
- Imaged for each pointing (using time synthesis)
- Lines below shows results for different frequencies
- Note: normalization by I does not correct Q,U,V

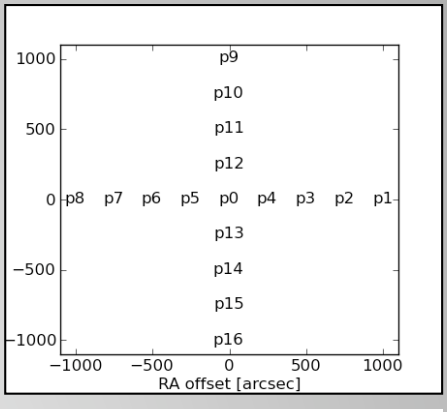

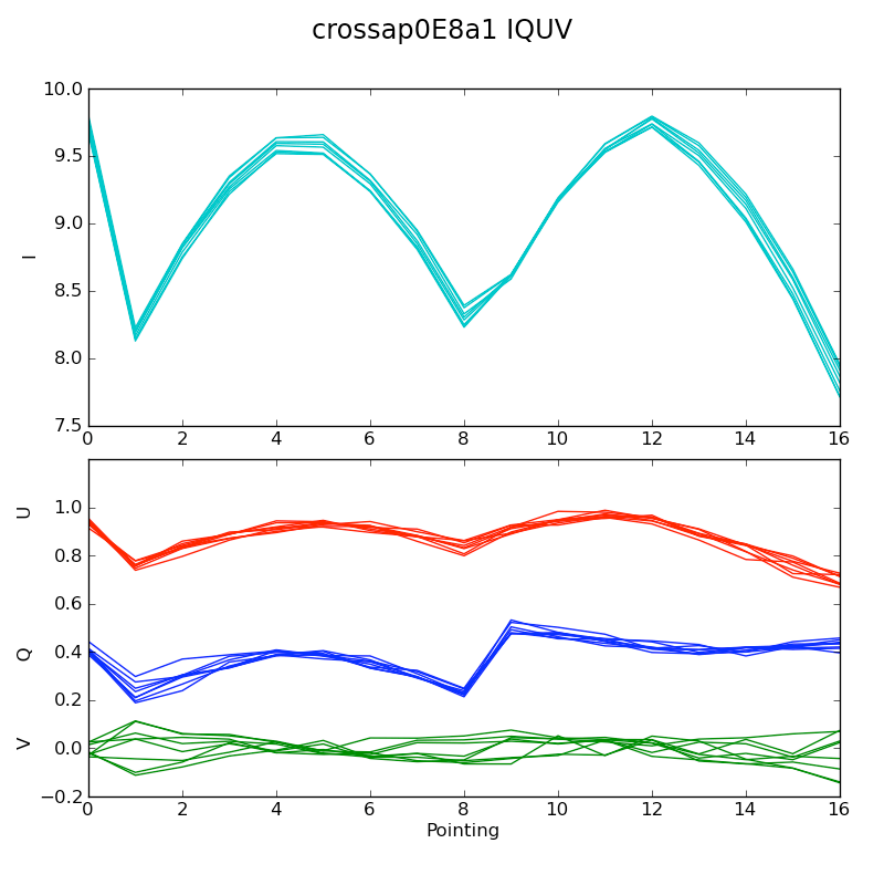

Calibrated for pointing 0 only

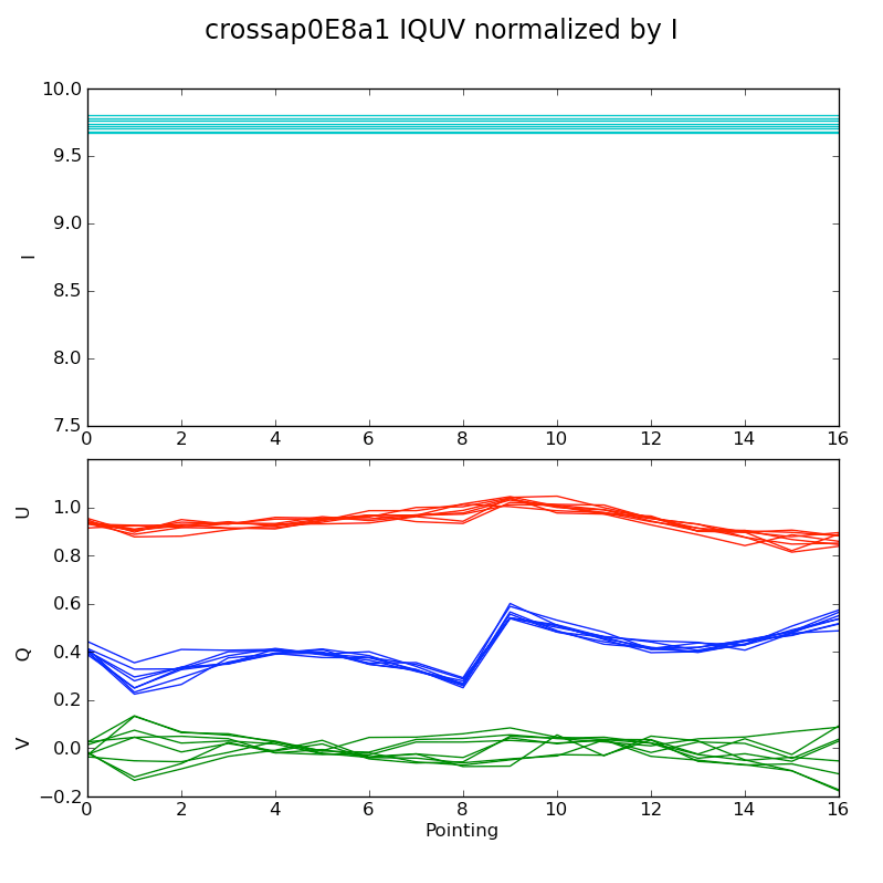

Q,U,V normalized by I

Faceting solution for IQUV by calibrating all pointings

- Calibrating for each pointing improves Q,U,V significantly
- So if the leakage solutions per pointing are smoothly varying and is predictable, one could possibly image subfields individually.
- Note: subtle errors in U seem to persist most noticeably at pointing 9
- Next: look at per-pointing leakage solutions

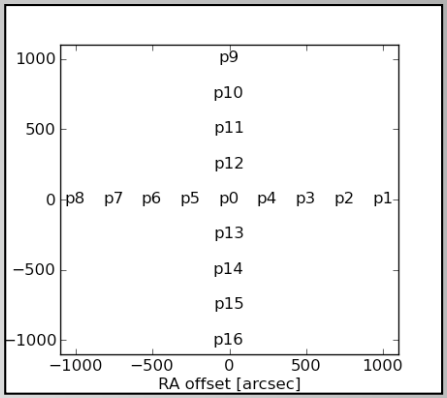

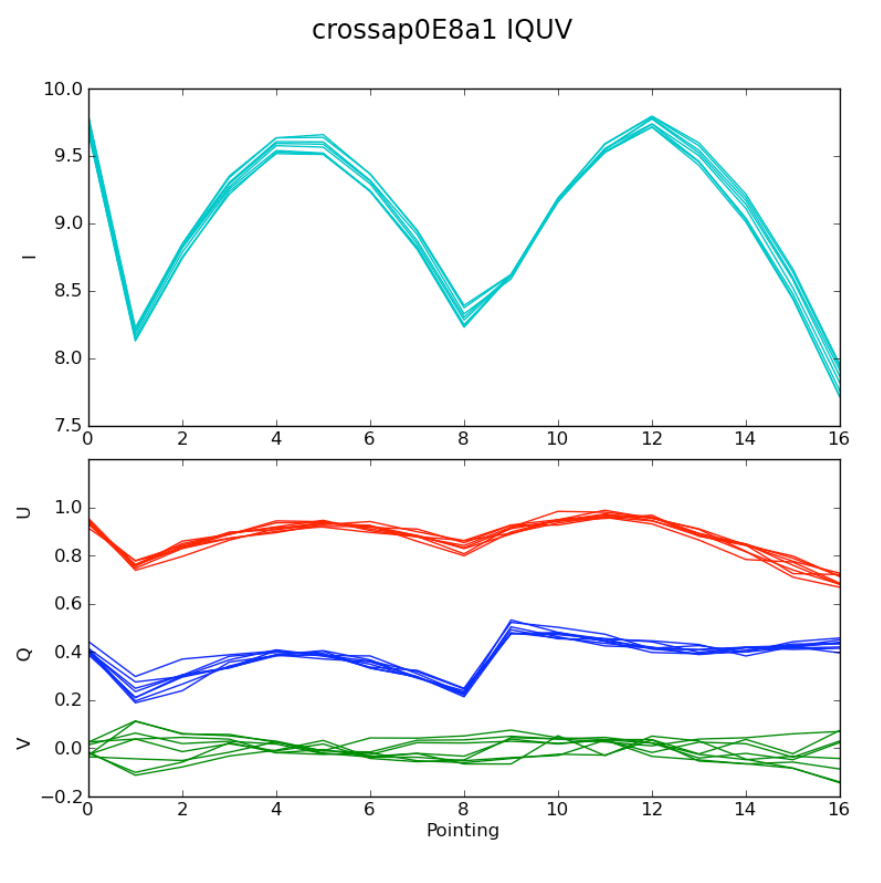

Calibrated for pointing 0 only

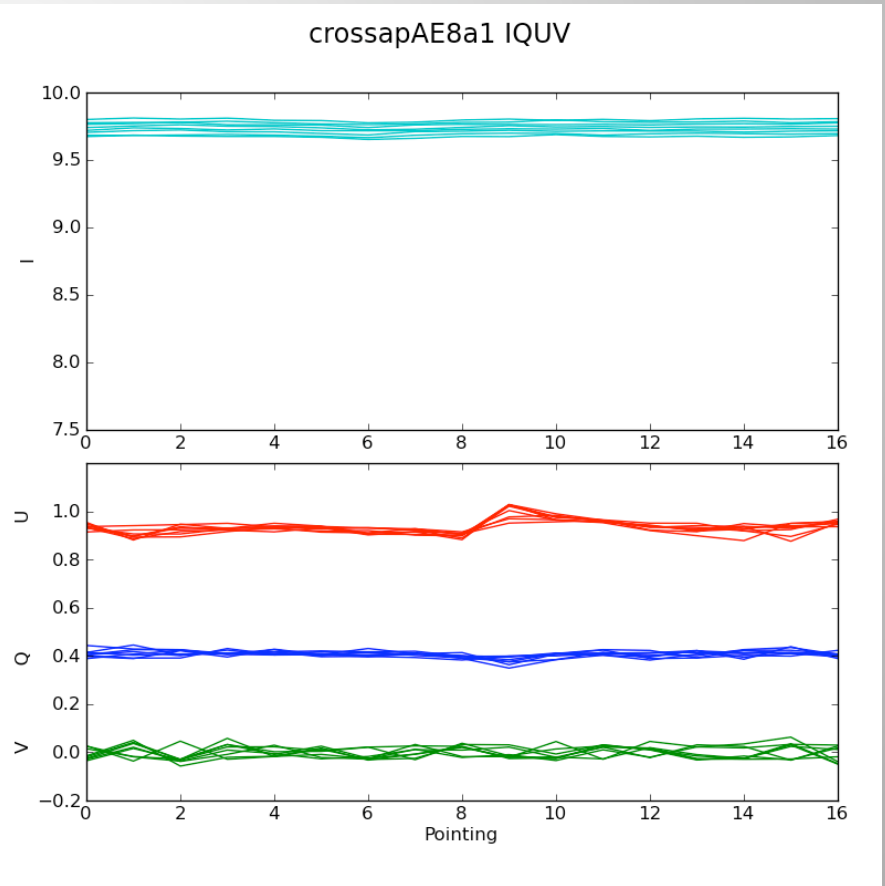

Calibrated for each pointing

Leakage per pointing, antenna, frequency

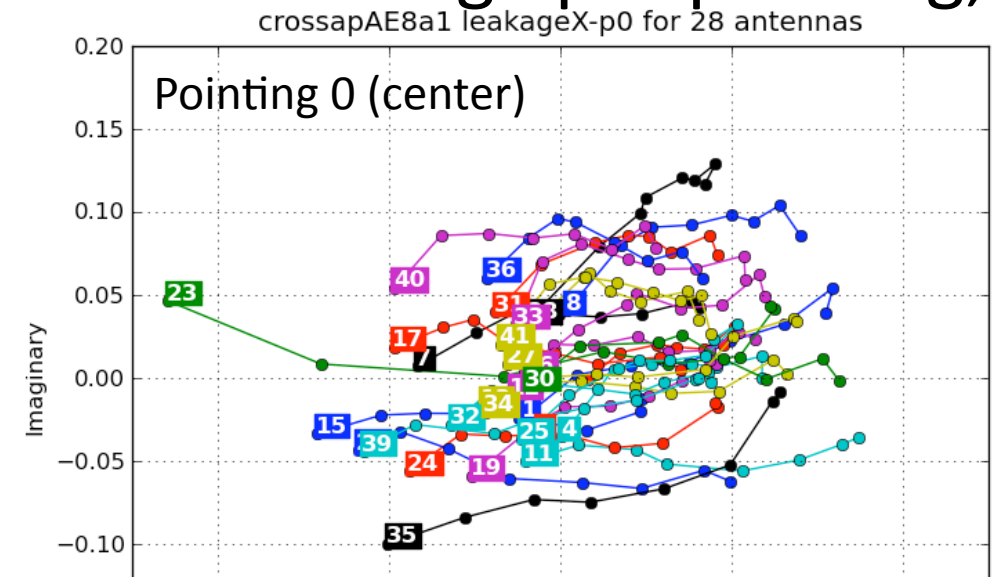

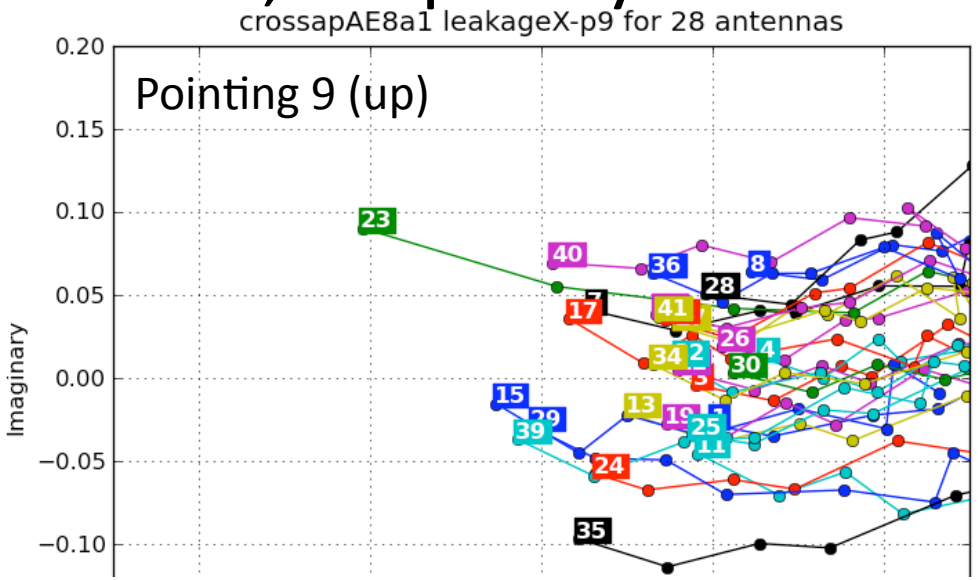

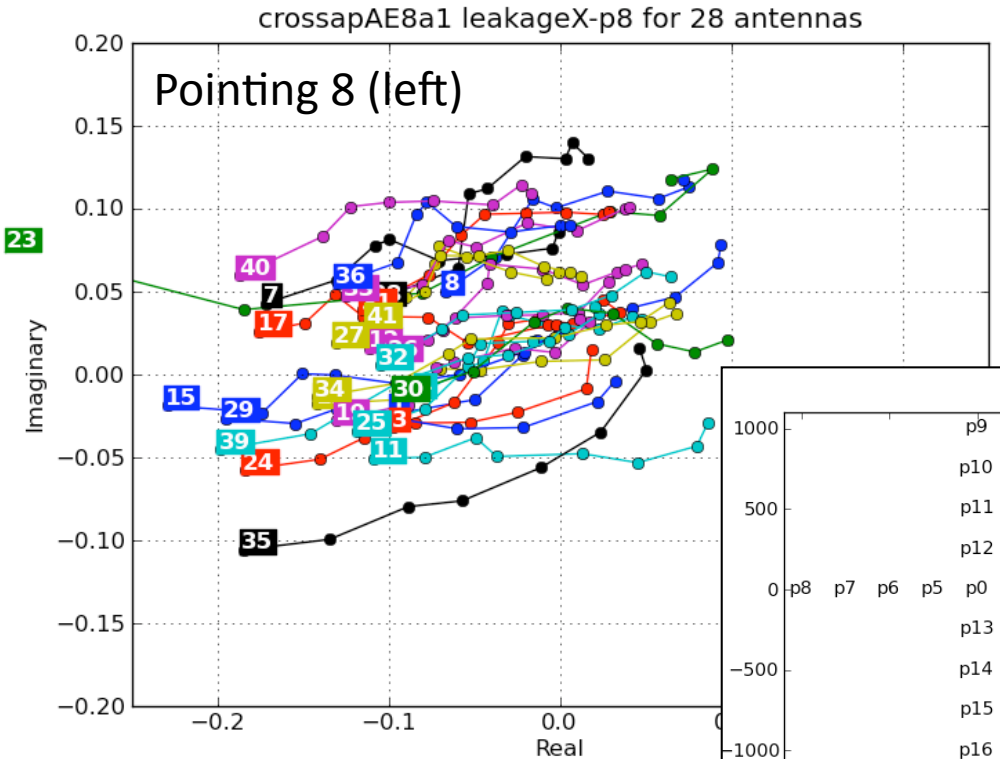

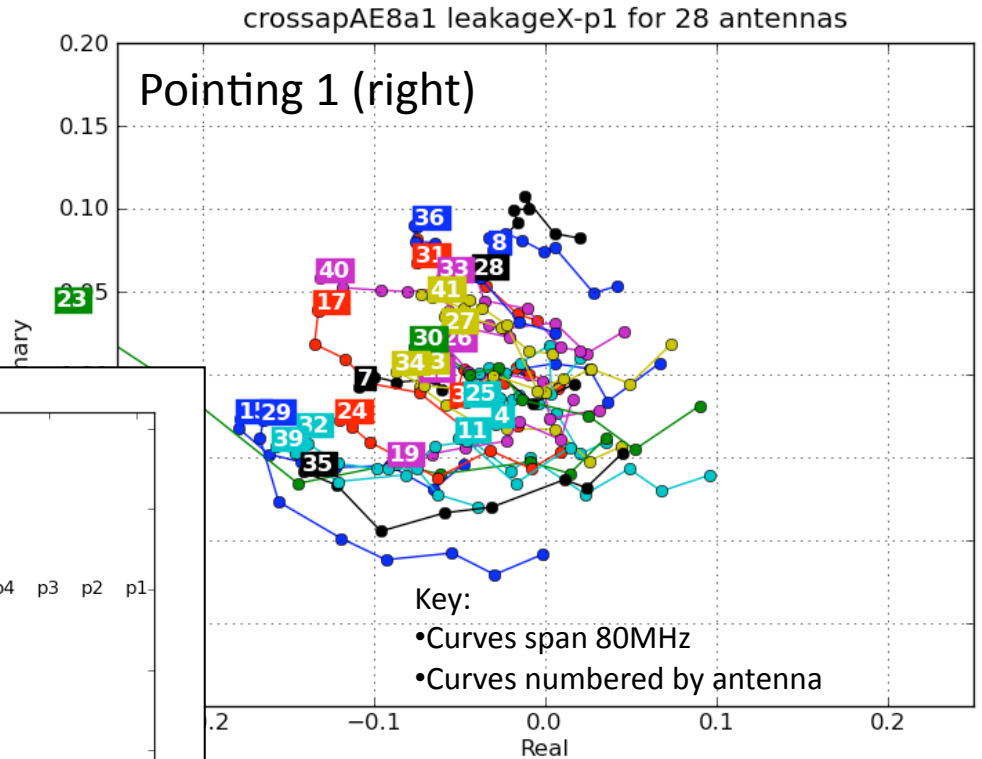

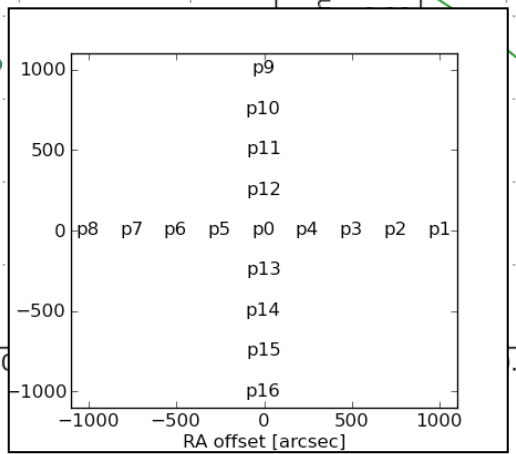

Key:

- Curves span 80MHz
- Curves numbered by antenna

Leakage per antenna, pointing, frequency

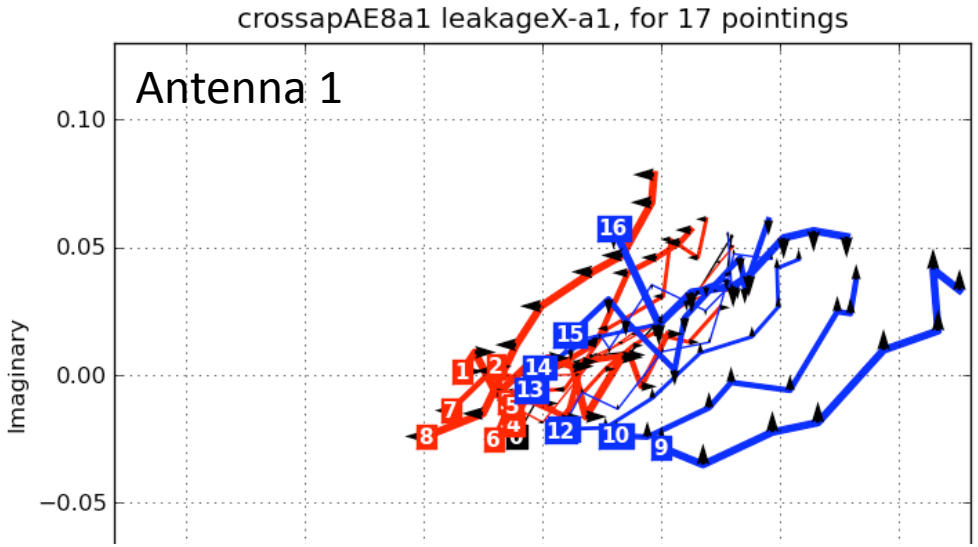

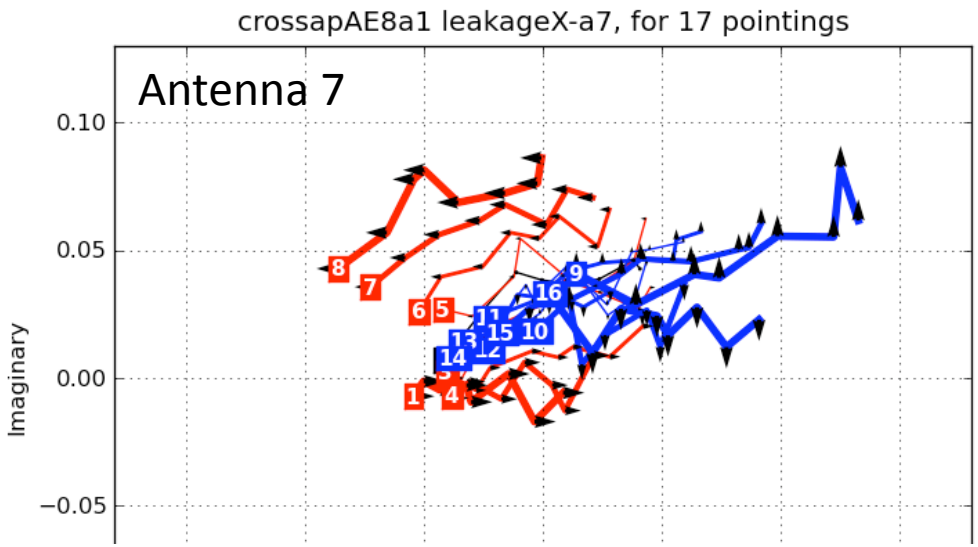

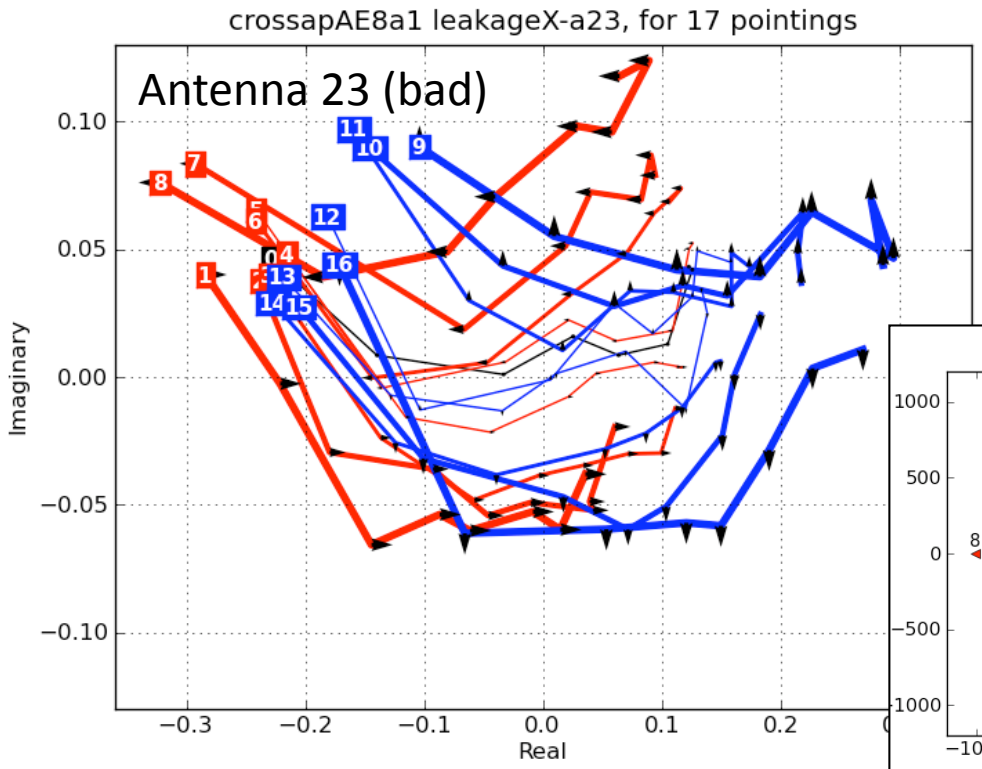

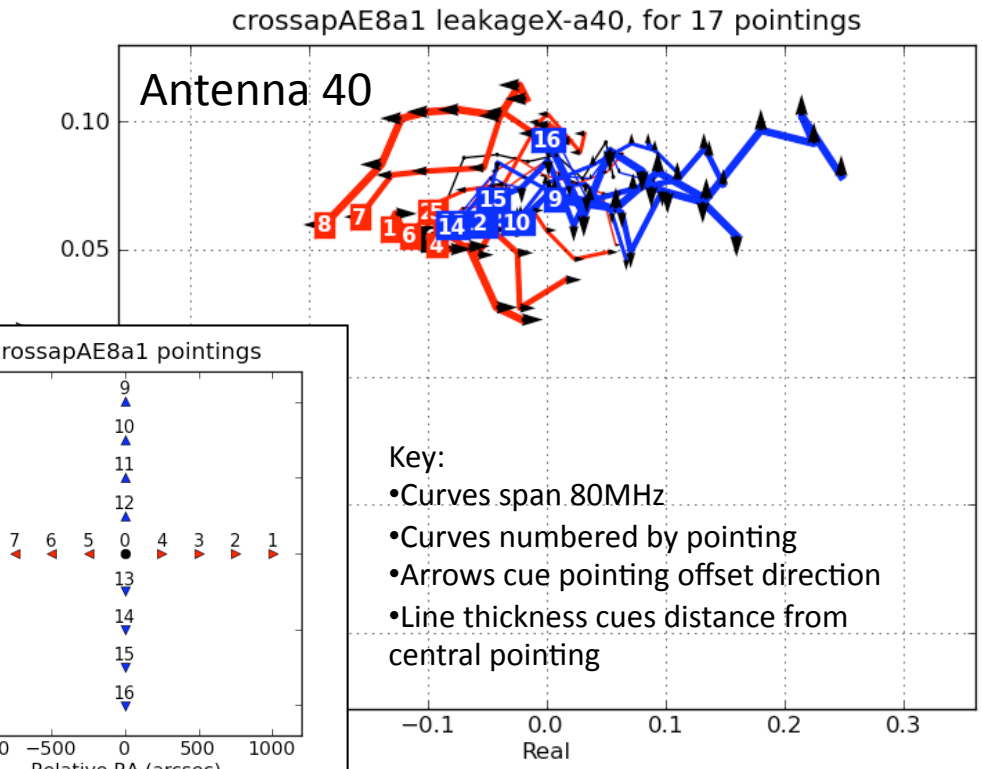

Key:

- Curves span 80MHz
- Curves numbered by pointing
- Arrows cue pointing offset direction
- Line thickness cues distance from central pointing

Parallactic angle effects on IQUV

- Calibrated for pointing 0 only; calibration solution applied to other pointings
- Each 50s scan is imaged independently (shown as different line below)
- Frequency results are averaged here over the 80MHz bandwidth
- Results are colour-coded by parallactic angle
- Component of Stokes I appears superimposed onto U, V with clear parallactic angle dependency

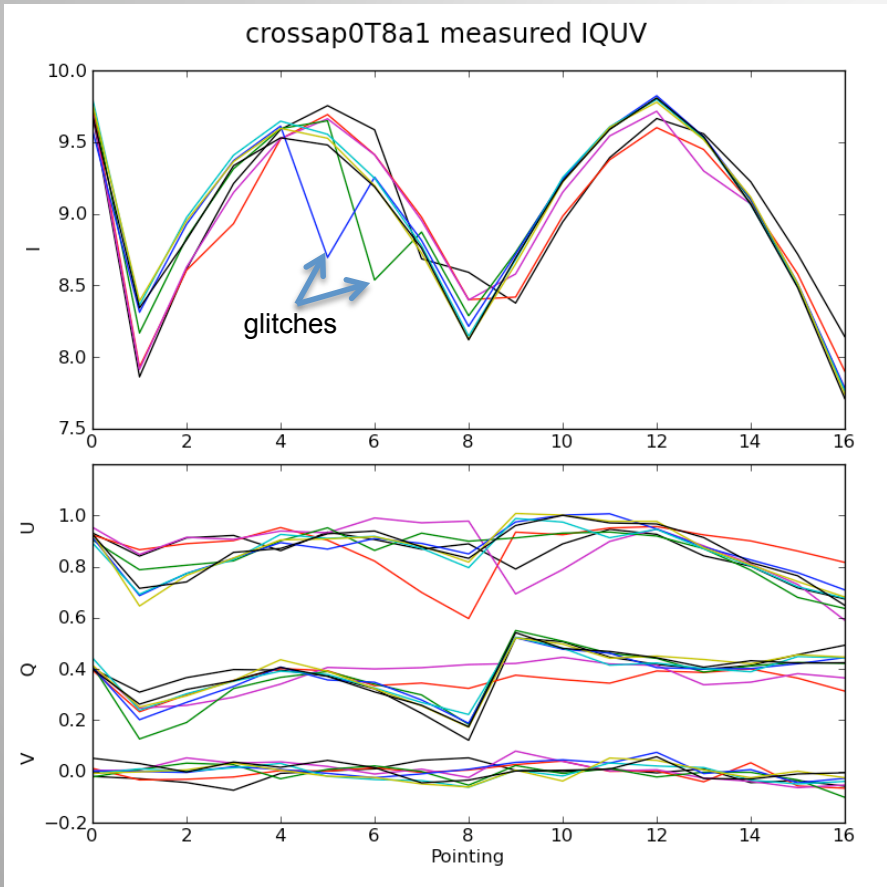

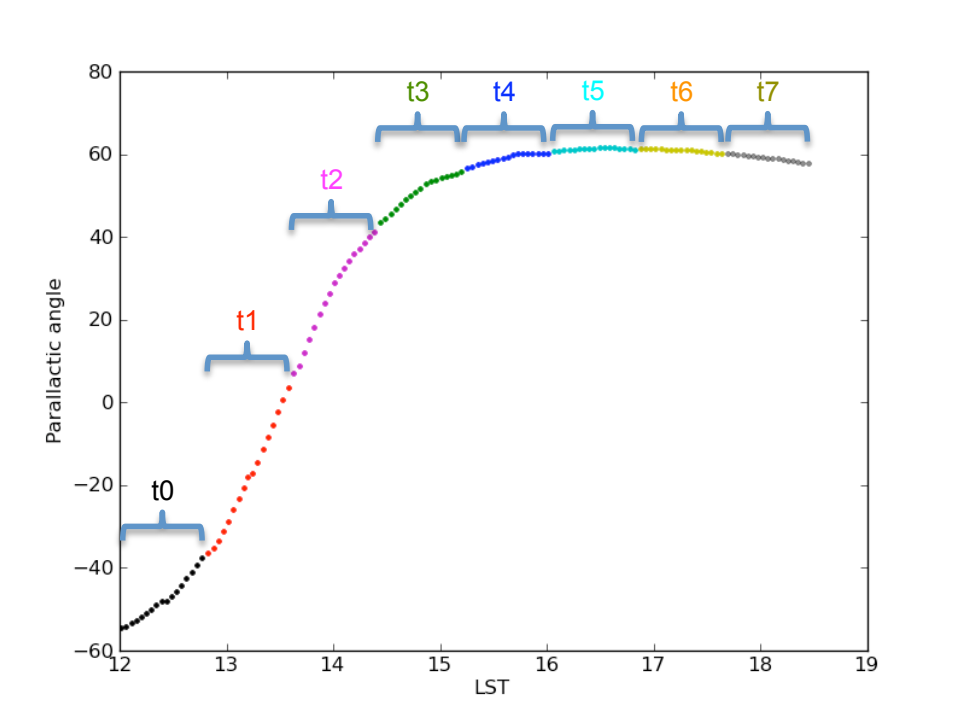

Relative AZ EL plane

- Plane is stationary with respect to the primary beam
- Data points fill out the plane
- Multiple data points occur at the same point in the plane
- Note that the same off center pointing samples different parts of the primary beam during the course of the observation

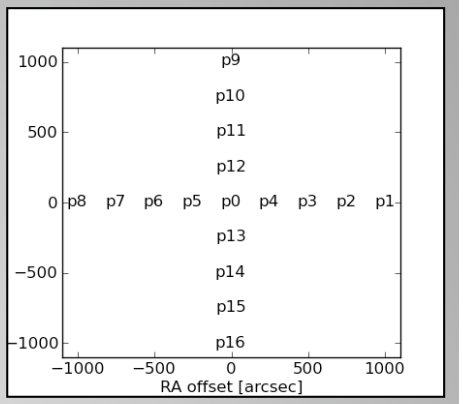

$$HA_{p,t} = LST_t - RA_p$$

$$\sin(EL_{p,t}) = \sin(DEC_p)\sin(LAT) + \cos(DEC_p)\cos(LAT)\cos(HA_{p,t})$$

$$\tan(AZ_{p,t}) = \frac{-\sin(HA_{p,t})\cos(DEC_p)}{\sin(DEC_p)\cos(LAT) - \cos(DEC_p)\sin(LAT)\cos(HA_{p,t})}$$

$$\tan(\chi_{p,t}) = \frac{\sin(HA_{p,t})\cos(LAT)}{\sin(LAT)\cos(DEC_p) - \sin(DEC_p)\cos(LAT)\cos(HA_{p,t})}$$

$$EL_{rel,p,t} = EL_{p,t} - EL_{0,t}$$

$$AZ_{rel,p,t} = AZ_{p,t} - AZ_{0,t}$$

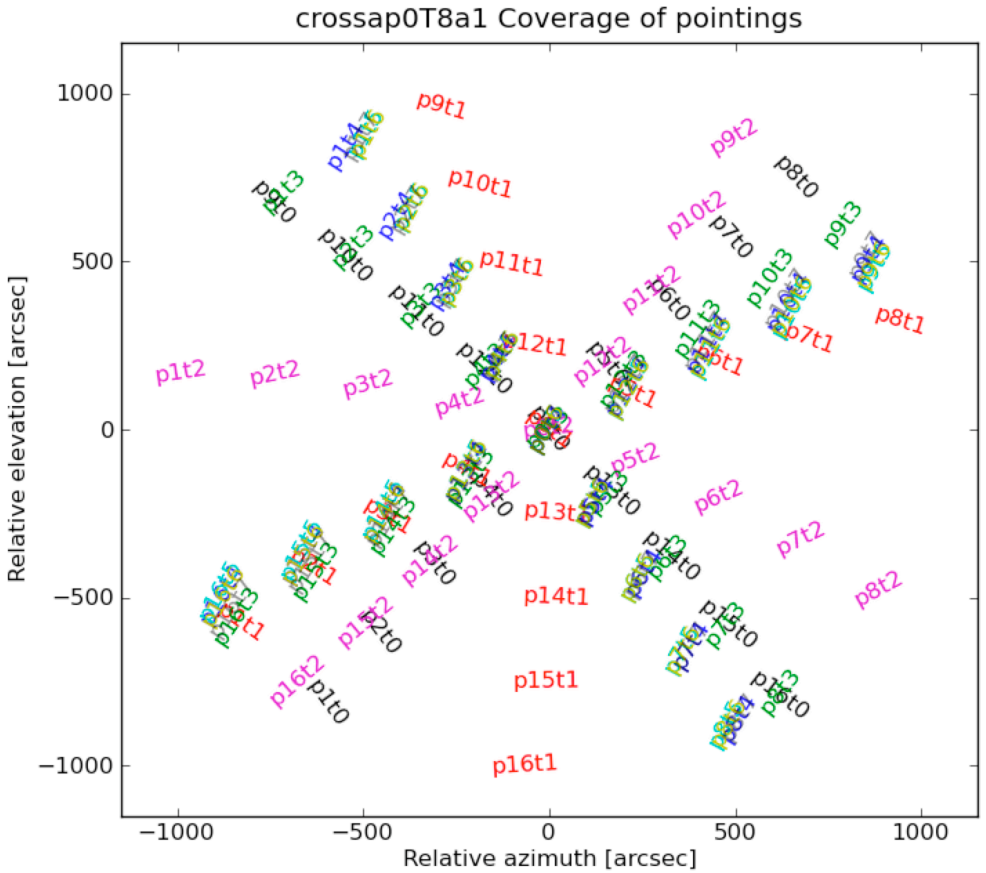

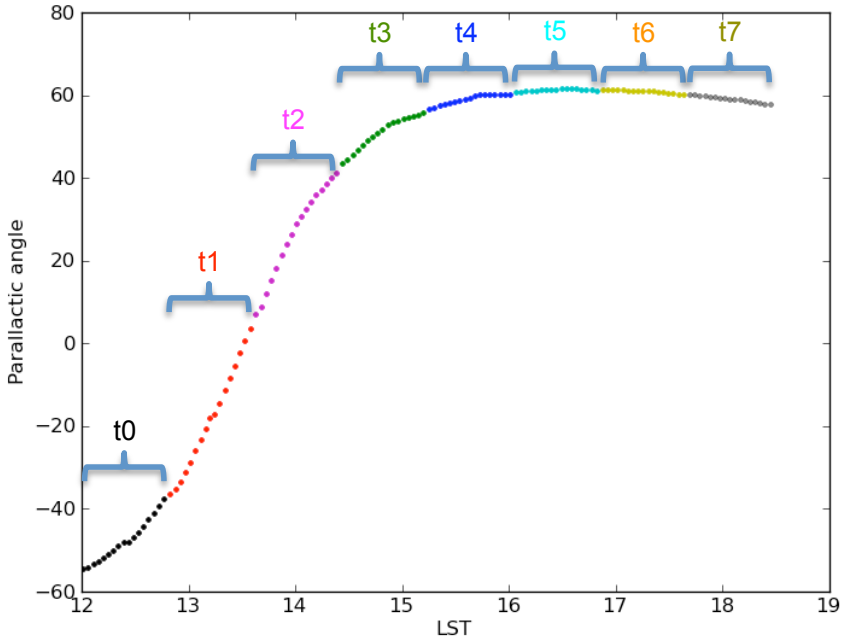

Derotating the QU error

- The errors between the measured Q,U values and true Q,U values of the calibrator is displayed below as position angle vectors
- Derotating the position angle by the parallactic angle gives smoothly varying, self-consistent results

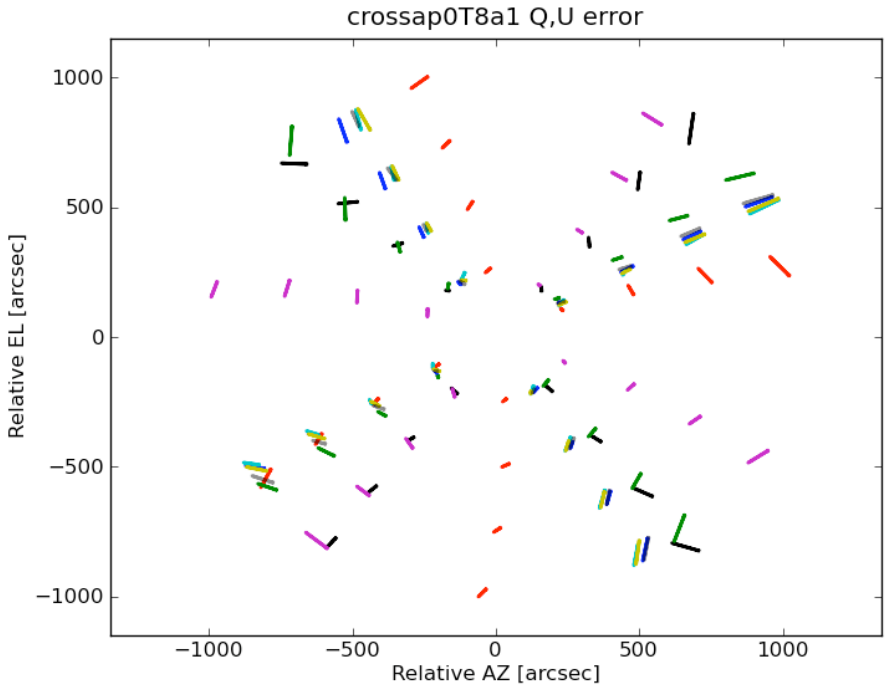

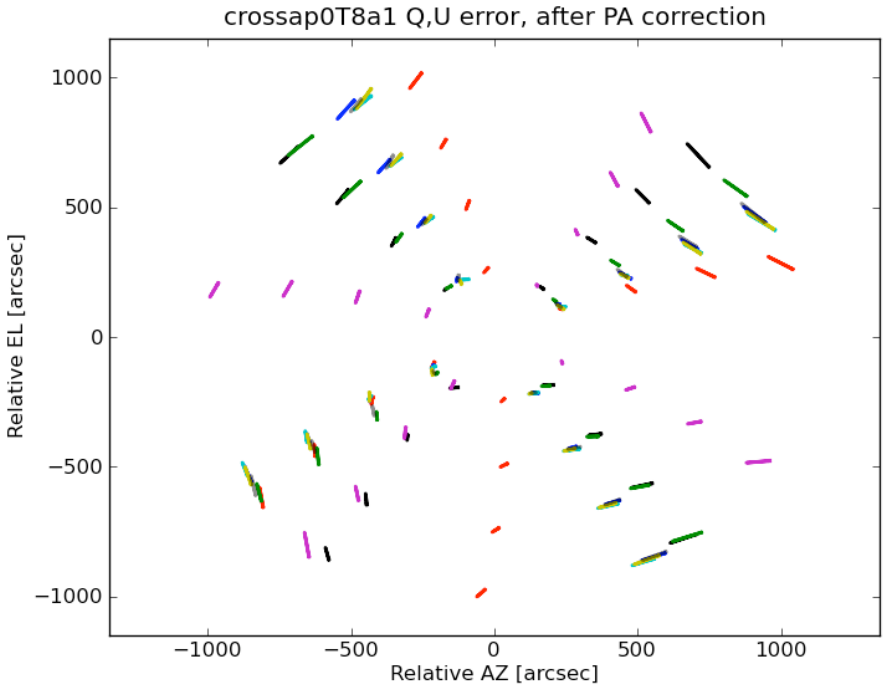

Theory

- Neglecting higher order terms (in gain errors ε and leakages D) it can be shown that the measured $\vec{IQUV}$ values relate to the true IQUV values as below
- The equation shows how the components ζ_{pp} and ε_{np} of Stokes I is rotated into Q and U as a function of parallactic angle

$$\begin{bmatrix} \vec{I} \\ \vec{Q} \\ \vec{U} \\ \vec{V} \end{bmatrix} = \begin{bmatrix} \frac{1}{2}\varepsilon_{pp}+1 & \frac{1}{2}\cdot(-\zeta_{pp}\cdot\sin(2\cdot\chi)+\varepsilon_{np}\cdot\cos(2\cdot\chi)) & \frac{1}{2}\cdot(\zeta_{pp}\cdot\cos(2\cdot\chi)+\varepsilon_{np}\cdot\sin(2\cdot\chi)) & -\frac{1}{2}\zeta_{nn}\mathrm{j} \\ \frac{1}{2}\cdot(-\zeta_{pp}\cdot\sin(2\cdot\chi)+\varepsilon_{np}\cdot\cos(2\cdot\chi)) & \frac{1}{2}\varepsilon_{pp}+1 & \frac{1}{2}\zeta_{np} & \frac{1}{2}\cdot(-\zeta_{pn}\cdot\cos(2\cdot\chi)-\varepsilon_{nn}\cdot\sin(2\cdot\chi))\,\mathrm{j} \\ \frac{1}{2}\cdot(\zeta_{pp}\cdot\cos(2\cdot\chi)+\varepsilon_{np}\cdot\sin(2\cdot\chi)) & -\frac{1}{2}\zeta_{np} & \frac{1}{2}\varepsilon_{pp}+1 & \frac{1}{2}\cdot(-\zeta_{pn}\cdot\sin(2\cdot\chi)+\varepsilon_{nn}\cdot\cos(2\cdot\chi))\,\mathrm{j} \\ -\frac{1}{2}\zeta_{nn}\mathrm{j} & \frac{1}{2}\cdot(\zeta_{pn}\cdot\cos(2\cdot\chi)+\varepsilon_{nn}\cdot\sin(2\cdot\chi))\,\mathrm{j} & \frac{1}{2}\cdot(\zeta_{pn}\cdot\sin(2\cdot\chi)-\varepsilon_{nn}\cdot\cos(2\cdot\chi))\,\mathrm{j} & \frac{1}{2}\varepsilon_{pp}+1 \end{bmatrix} \cdot \begin{bmatrix} I \\ Q \\ U \\ V \end{bmatrix}$$

Where the direction dependent terms are:

$$\begin{aligned}
\epsilon_{pp} &= \epsilon_{x1} + \epsilon_{y1} + \epsilon^*_{x2} + \epsilon^*_{y2} \\
\epsilon_{nn} &= \epsilon_{x1} - \epsilon_{y1} - \epsilon^*_{x2} + \epsilon^*_{y2} \\
\epsilon_{np} &= \epsilon_{x1} - \epsilon_{y1} + \epsilon^*_{x2} - \epsilon^*_{y2} \\
\zeta_{np} &= D_{x1} - D_{y1} + D^*_{x2} - D^*_{y2} \\
\zeta_{pn} &= D_{x1} + D_{y1} - D^*_{x2} - D^*_{y2} \\
\zeta_{nn} &= D_{x1} - D_{y1} - D^*_{x2} + D^*_{y2} \\
\zeta_{pp} &= D_{x1} + D_{y1} + D^*_{x2} + D^*_{y2}
\end{aligned}$$

$$\vec{g}_{x1} = g_{x1}\cdot(1+\varepsilon_{x1})$$

Solving direction dependent ε ζ terms

- Can re-arrange equations and solve by matrix inversion
- Model using quadratics or constants (equations not shown)
- Weigh each equation to define solution neighbourhoods
- Can also calculate directly ε_{pp} (not shown) but then sensitive to glitches

$$\begin{bmatrix} \vec{I} \\ \vec{Q} \\ \vec{U} \\ \vec{V} \end{bmatrix} = \begin{bmatrix} I & Q\cos(2\chi)+U\sin(2\chi) & 0 & U\cos(2\chi)-Q\sin(2\chi) & 0 & 0 & -V \\ Q & I\cos(2\chi) & U & -I\sin(2\chi) & -V\sin(2\chi) & -V\cos(2\chi) & 0 \\ U & I\sin(2\chi) & -Q & I\cos(2\chi) & V\cos(2\chi) & -V\sin(2\chi) & 0 \\ V & 0 & 0 & 0 & Q\sin(2\chi)-U\cos(2\chi) & Q\cos(2\chi)+U\sin(2\chi) & -I \end{bmatrix} \begin{bmatrix} \frac{1}{2}\varepsilon_{pp}+1 \\ \frac{1}{2}\varepsilon_{np} \\ \frac{1}{2}\zeta_{np} \\ \frac{1}{2}\zeta_{pp} \\ \frac{1}{2}\varepsilon_{nn} \\ \frac{1}{2}\zeta_{pn} \\ \frac{1}{2}\zeta_{nn} \end{bmatrix}$$

$$w_i(AZ_{rel}, EL_{rel}) = \exp\left[-\frac{1}{2}\frac{(AZ_{rel,i} - AZ_{rel})^2 + (EL_{rel,i} - EL_{rel})^2}{\sigma^2}\right]$$

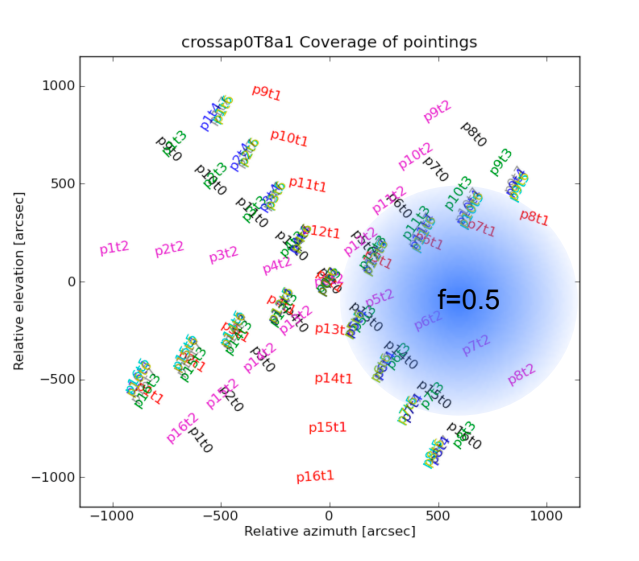

$$\begin{aligned} a &= B \cdot c \\ W \cdot a &= W \cdot B \cdot c \\ c &= (W \cdot B)^{-1} \cdot W \cdot a \end{aligned}$$

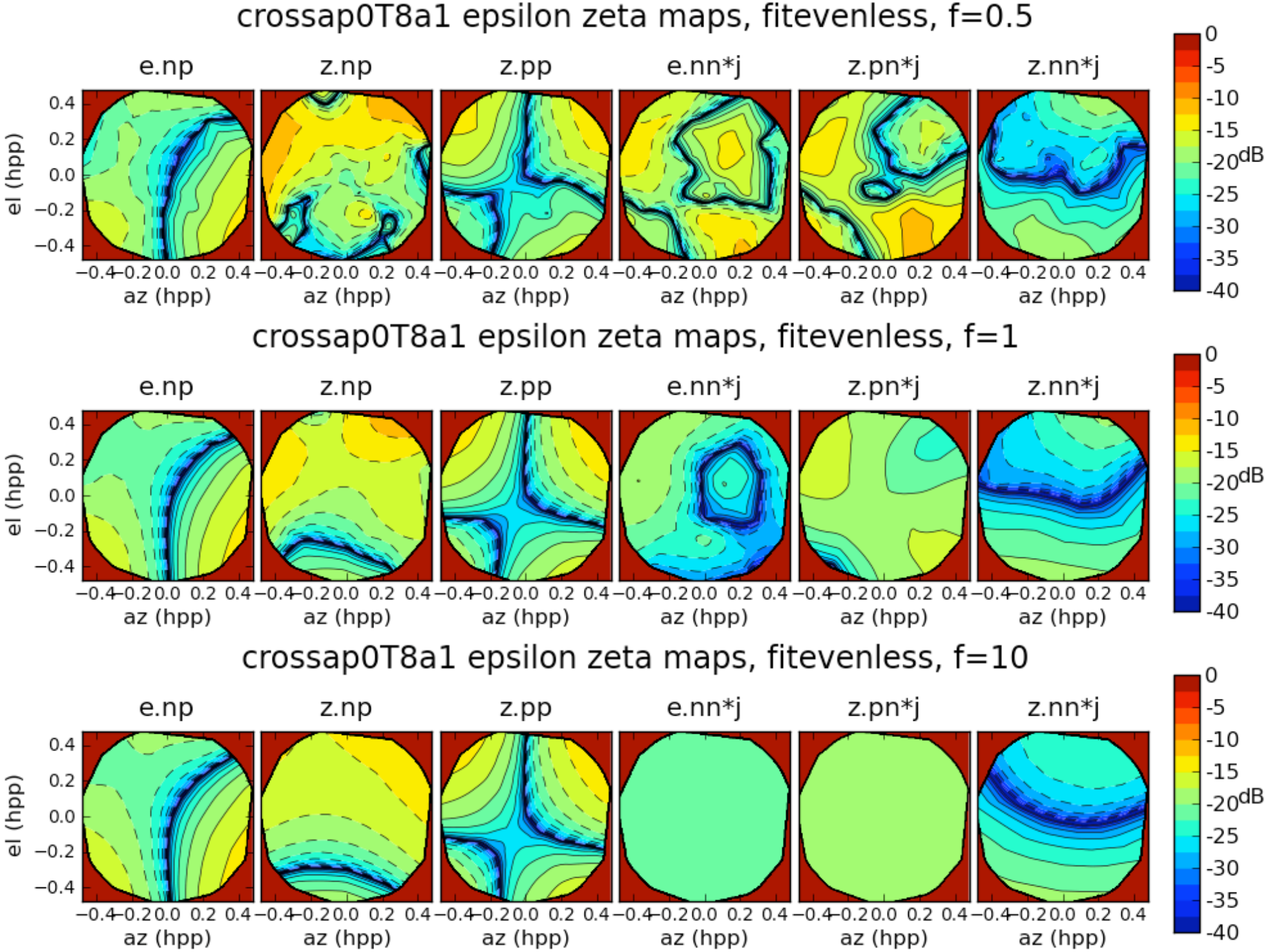
crossap0T8a1 epsilon zeta maps, fitevenless, f=0.5
crossap0T8a1 epsilon zeta maps, fitevenless, f=1
crossap0T8a1 epsilon zeta maps, fitevenless, f=10
e.np
z.np
z.pp
e.nn*j
z.pn*j
z.nn*j
el (hpp)
az (hpp)
0.4
0.2
0.0
−0.2
−0.4
−0.4 −0.2 0.0 0.2 0.4
0
-5
-10
-15
-20
-25
-30
-35
-40
dB

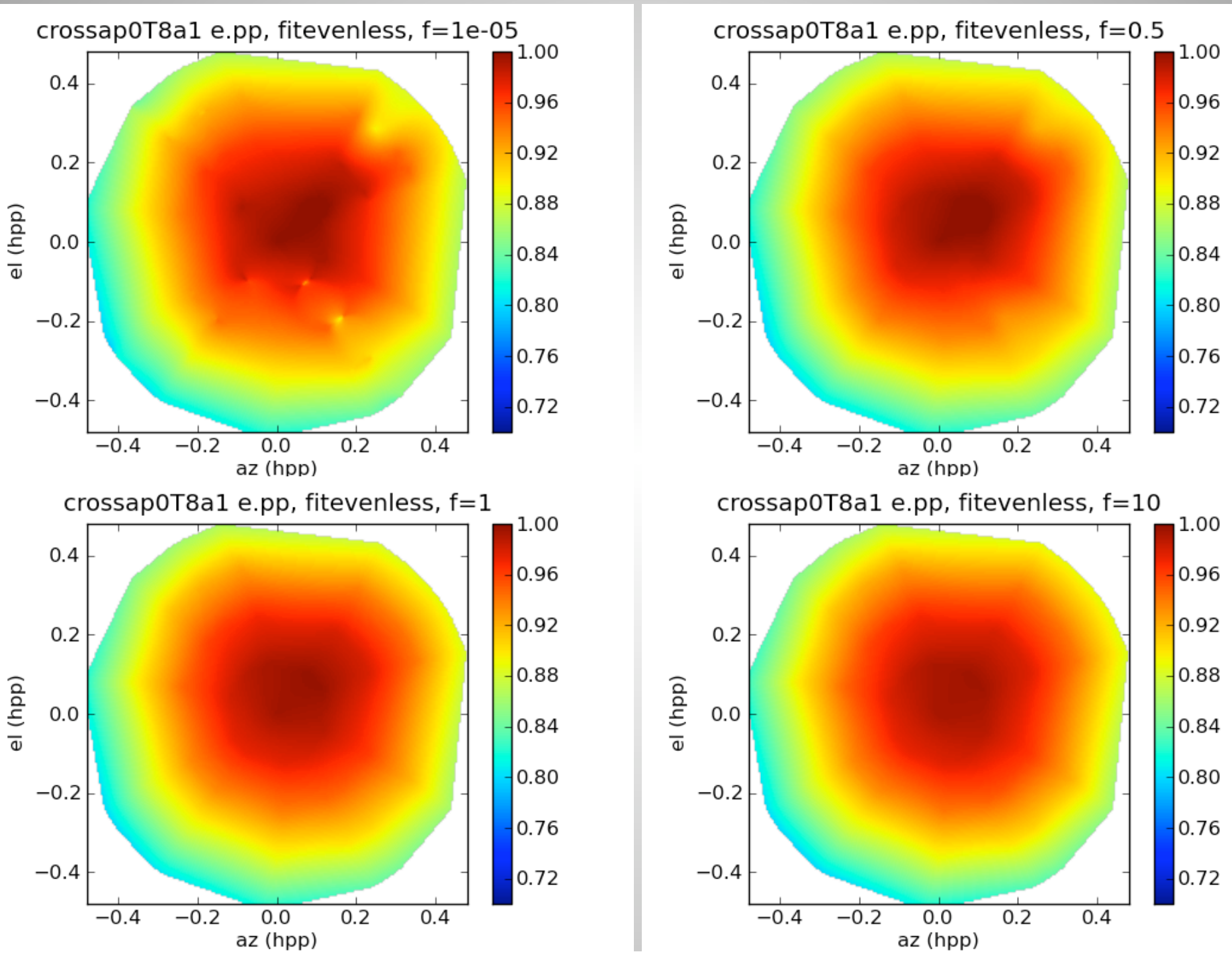
crossap0T8a1 e.pp, fitevenless, f=1e-05
crossap0T8a1 e.pp, fitevenless, f=0.5
crossap0T8a1 e.pp, fitevenless, f=1
crossap0T8a1 e.pp, fitevenless, f=10
el (hpp)
az (hpp)
0.4
0.2
0.0
−0.2
−0.4
1.00
0.96
0.92
0.88
0.84
0.80
0.76
0.72

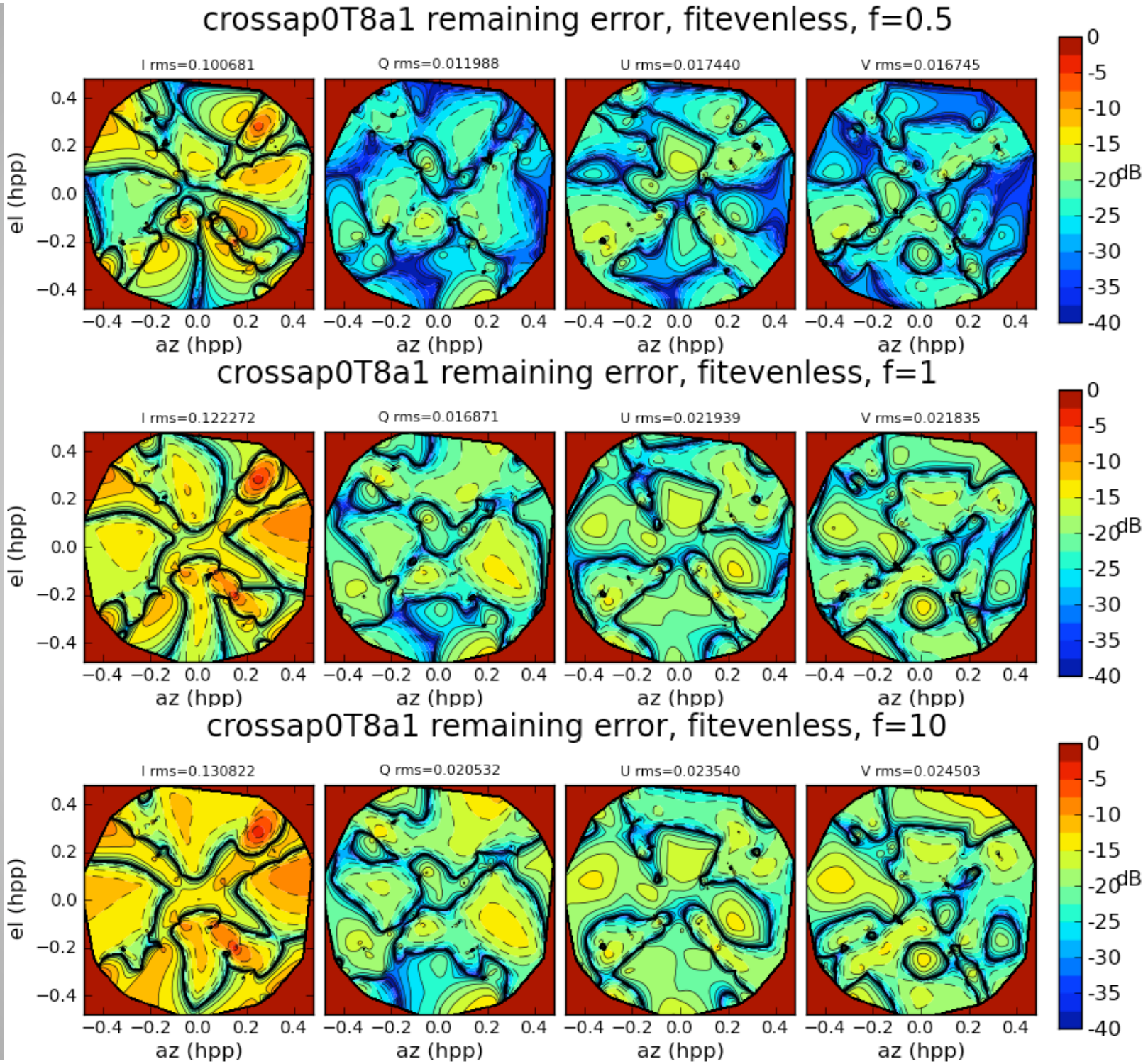
crossap0T8a1 remaining error, fitevenless, f=0.5
I rms=0.100681
Q rms=0.011988
U rms=0.017440
V rms=0.016745
crossap0T8a1 remaining error, fitevenless, f=1
I rms=0.122272
Q rms=0.016871
U rms=0.021939
V rms=0.021835
crossap0T8a1 remaining error, fitevenless, f=10
I rms=0.130822
Q rms=0.020532
U rms=0.023540
V rms=0.024503
el (hpp)
az (hpp)
dB
0
-5
-10
-15
-20
-25
-30
-35
-40
0.4
0.2
0.0
−0.2
−0.4

Uncorrected

Effectively normalized by Stokes I

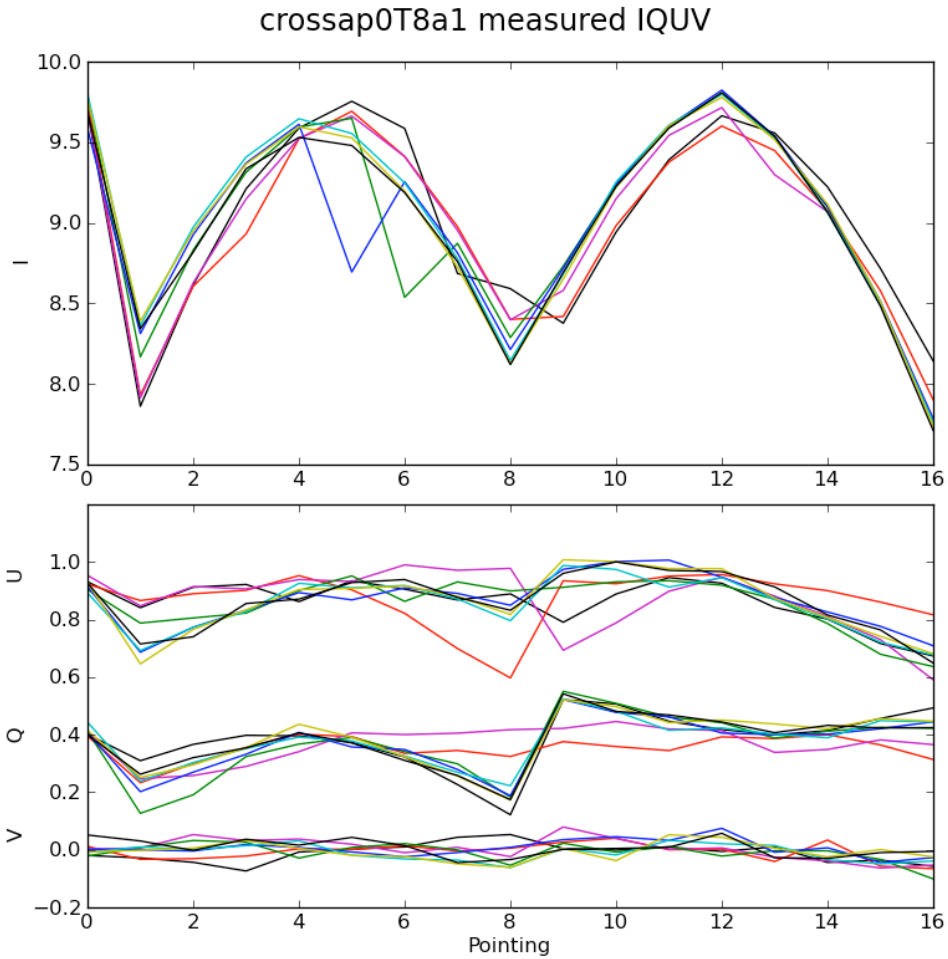

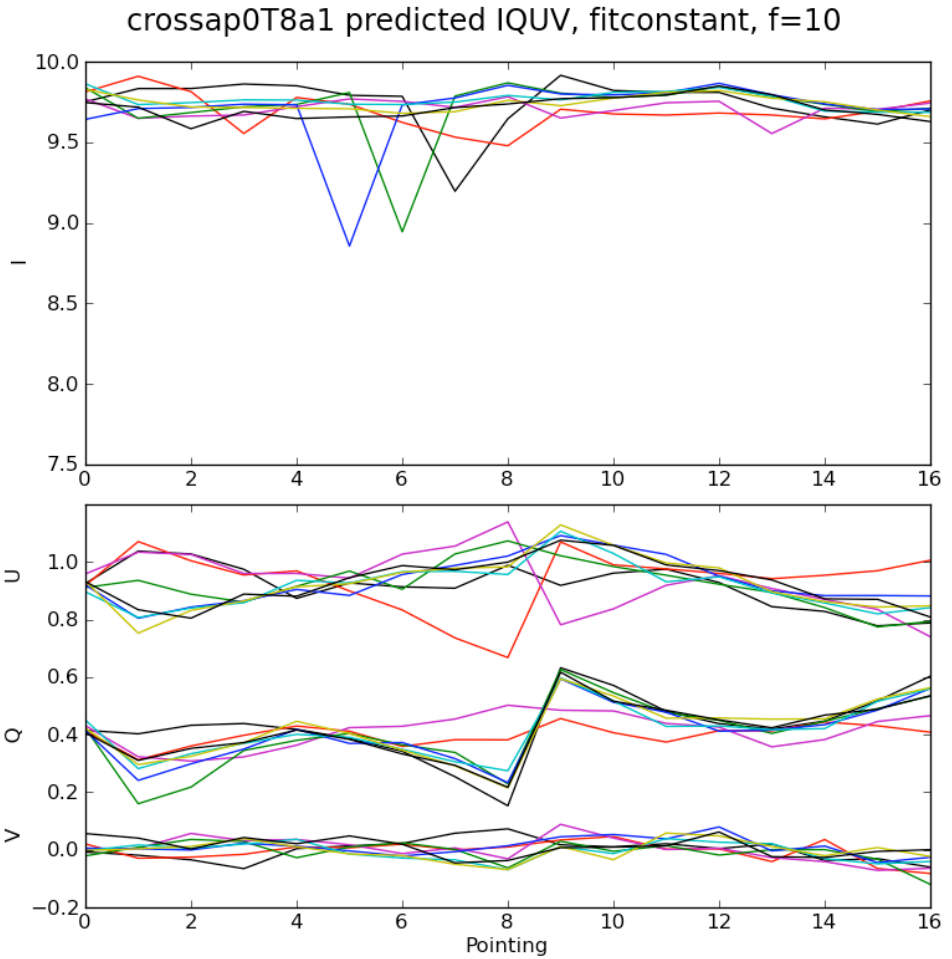

Quadratic model for ε_{pp} only,
constants for other dir dep terms

Effectively normalized by Stokes I

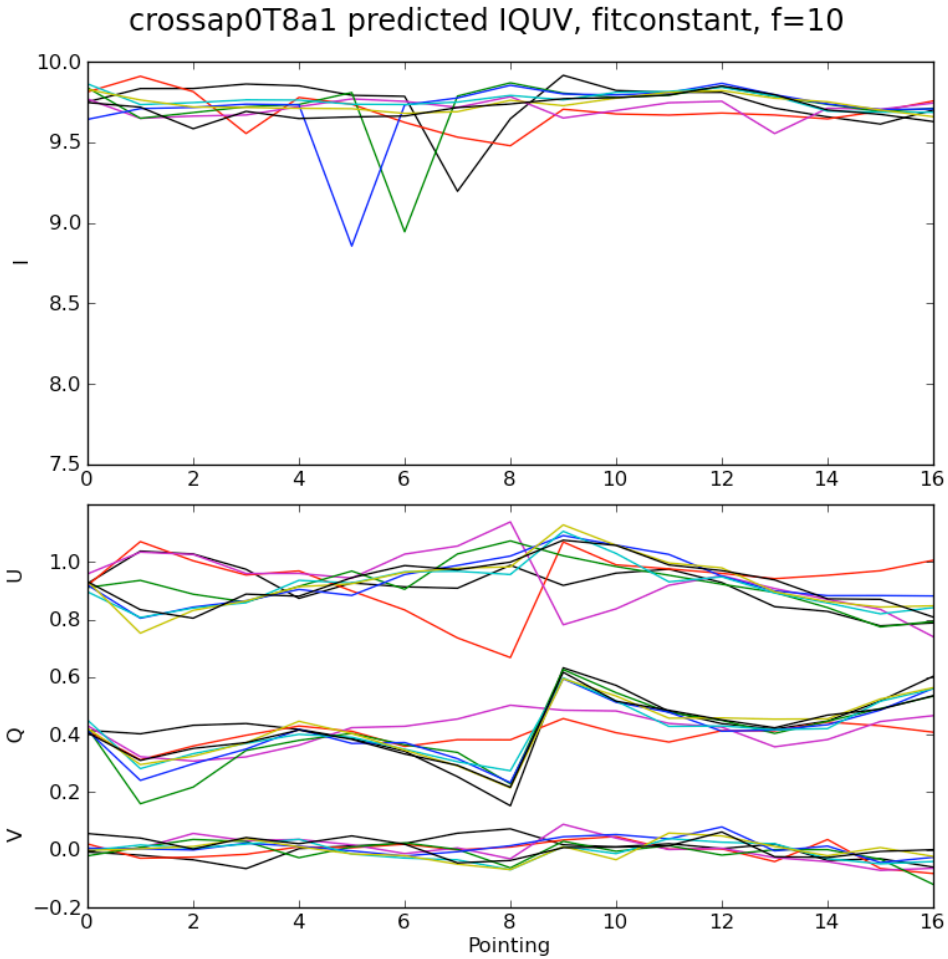

RMS errors of
1.37% 0.96% 0.88% 0.36%
in I Q U V
respectively wrt true Stokes I

Quadratic models for dir dept terms

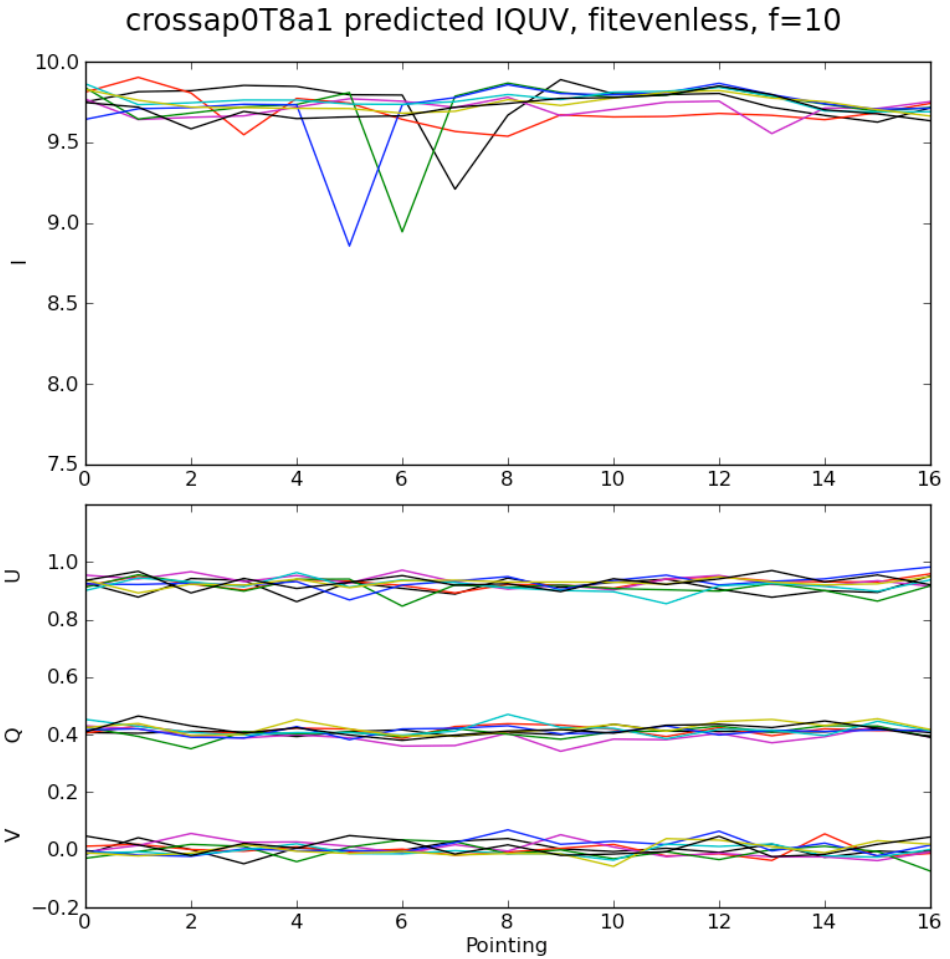

RMS errors of
1.35% 0.21% 0.24% 0.25%
in I Q U V
respectively wrt true Stokes I

Summary

- Faceting:
  - Leakages become large when calibrating for off-center pointings (assumptions used in Miriad's solver becomes invalid, and solving sometimes fails)
  - There are some trends in leakage solutions but they vary per antenna as a function of frequency and pointing direction in a non-trivial way
  - This method could be pursued further, but
  - Any off-center pointing samples different parts of the primary beam during the course of the observation. The off-center cross polarization components (in particular) of the primary beam are not at all circularly symmetric. This violates the solver's assumption that feed leakages are constant during the observation even though a best fit solution is still found.
- Image plane modeling and corrections:
  - The overall polarimetric response of the interferometer can be measured
  - Direction dependent terms can be modeled using simple quadratics up to at least half the distance to the the half power point of the primary beam
  - Prediction in the image plane using the model improves Q and U by a factor of about 4 across the field compared to simple normalization
  - The most straightforward correction implementation requires imaging in snap shot mode where images must be averaged after the correction
  - However it is possible to derive equivalent beam patterns for A-projection implementation
  - Per antenna solutions are possible (work in progress)
  - Not immediately suitable for large layouts where antennas experience different parallactic rotation
- More experimentation should be done to test stability of solutions over time, to develop a practical calibration strategy requiring only a few calibrator pointings
- The ATA is a great place to test new concepts and algorithms

Thanks to

- Geoffrey Bower, Jasper Horrel, Debra Sheperd and Ludwig Schwardt
- The Berkeley MMM group
- SKA SA